Elastase and matrix metalloproteinase inhibitors induce regression, and tenascin-C antisense prevents progression, of vascular disease

Kyle Northcote Cowan,[1] Peter Lloyd Jones,[2] and Marlene Rabinovitch[1]

[1]Division of Cardiovascular Research, Hospital for Sick Children; and Department of Laboratory Medicine and Pathobiology, University of Toronto; Toronto, Ontario, Canada, M5G 1X8
[2]Pediatric Cardiology Research Laboratory, Children's Hospital of Philadelphia and the University of Pennsylvania, Philadelphia, Pennsylvania 19104, USA

Address correspondence to: Marlene Rabinovitch, Division of Cardiovascular Research, Hospital for Sick Children, 555 University Avenue, Toronto, Ontario, Canada, M5G 1X8.
Phone: (416) 813-5918; Fax: (416) 813-7480; E-mail: mr@sickkids.on.ca.

Received for publication February 12, 1999, and accepted in revised form November 10, 1999.

Increased expression of the glycoprotein tenascin-C (TN) is associated with progression of clinical and experimental pulmonary hypertension. In cultured smooth muscle cells (SMCs) TN is induced by matrix metalloproteinases (MMPs) and amplifies the proliferative response to growth factors. Conversely, suppression of TN leads to SMC apoptosis. We now report that hypertrophied rat pulmonary arteries in organ culture, which progressively thicken in association with cell proliferation and matrix accumulation, can be made to regress by inhibiting either serine elastases or MMPs. This effect is associated with reduced TN, suppression of SMC proliferation, and induction of apoptosis. Selective repression of TN by transfecting pulmonary arteries with antisense/ribozyme constructs also induces SMC apoptosis and arrests progressive vascular thickening but fails to induce regression. This failure is related to concomitant expansion of a SMC population, which produces an alternative cell survival $\alpha_v\beta_3$ ligand, osteopontin (OPN), in response to pro-proliferative cues provided by a proteolytic environment. OPN rescues MMP inhibitor–induced SMC apoptosis, and $\alpha_v\beta_3$ blockade induces apoptosis in hypertrophied arteries. Our data suggest that proteinase inhibition is a novel strategy to induce regression of vascular disease because this overcomes the pluripotentiality of SMC-matrix survival interactions and induces coordinated apoptosis and resorption of matrix.

J. Clin. Invest. **105**:21–34 (2000).

Introduction

Pulmonary hypertension results from a variety of initiating stimuli. Its progression is associated with abnormal endothelial morphology and function (1), muscularization of normally nonmuscular peripheral arteries related to differentiation of pericytes (2), and medial hypertrophy and neointimal formation in muscular arteries, as a consequence of hypertrophy, proliferation, and migration of resident smooth muscle cells (SMCs) and increased production of extracellular matrix (ECM) components. These components include collagen, elastin, fibronectin (FN), and tenascin-C (TN) (1, 3, 4). Experimental models have successfully recapitulated many of these features (3, 5). We have provided evidence that endothelial alterations may allow extravasation of a serum factor capable of stimulating SMC production of a vascular serine elastase (6–9). In cultured SMCs, a consequence of elastase-mediated degradation of ECM is the liberation of matrix-bound SMC mitogens such as basic fibroblast growth factor (FGF-2) (8, 10, 11). This serine elastase, if similar to others such as leukocyte elastase, may also direct further matrix degradation in disease through the activation (12, 13) and/or expression (7, 10, 14, 15) of matrix metalloproteinases (MMPs), whose presence has been documented at sites of vascular remodeling (16, 17).

Increased MMP activity in cultured SMCs induces expression of the ECM glycoprotein TN (18), which has been described in vascular diseases (19) including clinical and experimental pulmonary hypertension (4, 20). Evaluation of the pathophysiologic role of TN in pulmonary hypertension revealed a relationship with SMC proliferation. Both in monocrotaline-induced (Mct-induced) hypertensive pulmonary arteries (PAs) and in PAs from patients with congenital heart disease, a progressive increase in TN expression correlated with proliferating SMCs (4, 20). Subsequent studies in cultured PA SMCs documented that TN amplifies the mitogenic response to FGF-2 and is a prerequisite for EGF-dependent SMC proliferation (20).

Further studies related the cellular mechanisms underlying MMP-dependent TN gene transcription to β_3 integrin ligation and induction of MAP kinase activity (21). TN-mediated SMC proliferation resulted from clustering of its cognate ($\alpha_v\beta_3$ integrin) receptors, leading to formation of specialized focal adhesions and consequent clustering and phosphorylation of growth factor receptors (18). Conversely, when

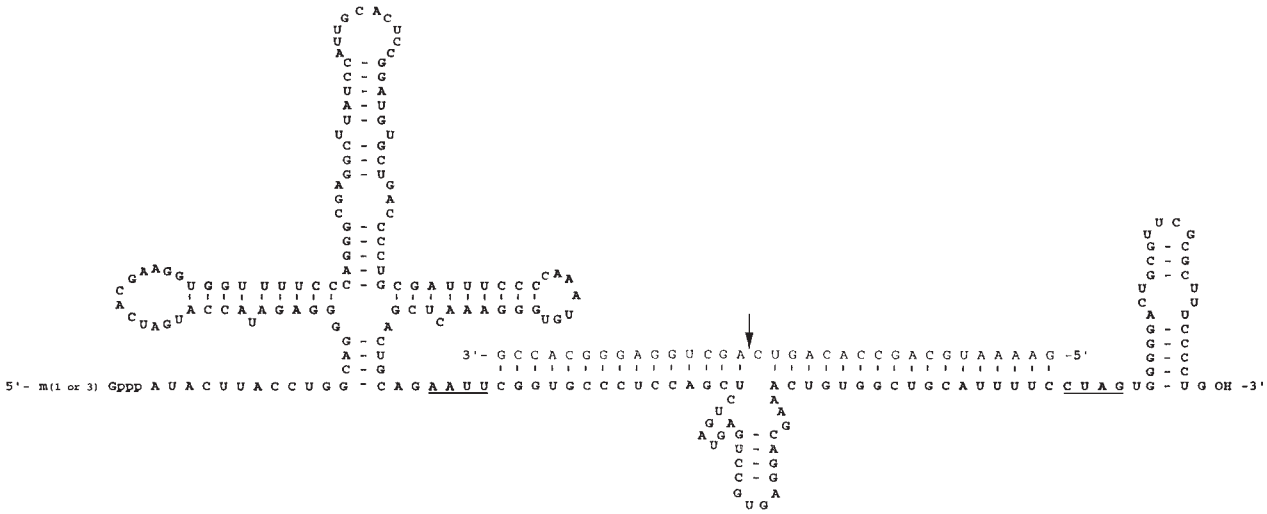

Figure 1

TN antisense cRNA. The hypothesized conformation of the TN antisense cRNA using the U1*Bam* pZeo mut *Eco*RI/*Spe*I expression vector backbone (schematic modified from ref. 27). The *Eco*RI and *Spe*I restriction sites are underlined. Hairpin loops at the 5′ and 3′ ends are shown, and the 32-bp antisense RNA described in the text is constructed to incorporate a hammerhead ribozyme such that it folds and hybridizes to the target TN mRNA at the location of the GUC consensus cleavage site (arrow, site of cleavage).

MMPs are inhibited either directly or by culturing SMCs on floating collagen gels, endogenous TN levels are markedly reduced, and SMC apoptosis is evident. Recent studies carried out in organ culture confirmed that SMCs in the hypertrophied PA responded similarly in attached and floating collagen gels and established that changes in elastase activity correlate with MMP activity (22).

We now show that direct inhibition of MMPs, including gelatinolytic activity attributable to MMP-2, or of serine elastases, leads to reduced TN, induction of apoptosis, loss of ECM, and regression of PA hypertrophy. Transfection of a TN antisense/ribozyme expression vector reduced TN mRNA and protein and resulted in considerable SMC apoptosis, although proliferation also occurred. This procedure arrested progressive hypertrophy, but failed to induce regression. Immunohistochemistry revealed an increase in osteopontin (OPN), an alternative $\alpha_v\beta_3$ ligand, possibly in response to cues provided by a proteolytic environment. We confirm that OPN functions as a survival factor rescuing SMCs from MMP inhibitor–induced apoptosis and that $\alpha_v\beta_3$ blockade can promote SMC apoptosis.

Methods

Preparation of explants. PAs were harvested from adult male Sprague-Dawley rats (300 g) (Charles River Laboratories, St. Laurent, Quebec, Canada) 21 days after a subcutaneous injection of 60 mg/kg of the alkaloid toxin Mct (Sigma Chemical Co., St. Louis, Missouri, USA) or an equal volume of saline in accordance with protocols approved by the Animal Care Committee of The Hospital for Sick Children. The rats were sacrificed, and PAs were excised and cultured in attached type I collagen gels as described previously (22).

Experimental designs. In the first set of experiments, organ cultures were supplemented with 1 of the following 3 proteinase inhibitors or with their administration vehicles. Administered were 6 mg/mL of the general serine elastase inhibitor alpha$_1$-proteinase inhibitor (α_1-PI; endotoxin-free Prolastin, a kind gift from M.A. Lark, Cutter Biologicals, Etobicoke, Ontario, Canada) in PBS, 8 μM of the synthetic MMP inhibitor GM-6001 (a kind gift from S. Sweidler, Glycomed, Alameda, California, USA) dissolved in 0.4% DMSO (Calbiochem-Novabiochem Corp., La Jolla, California, USA) or 0.8 μM of the selective neutrophil elastase inhibitor 1K (ZD0892; a kind gift from C. Veale, Zeneca Pharmaceuticals, Wilmington, Delaware, USA), delivered in 5% polyethylene glycol (PEG; Sigma Chemical Co.). Inhibitors were chosen to target MMPs or the heightened elastase activity demonstrated in Mct-induced vascular disease (8, 18, 21, 22). Doses were based upon our previous studies (11, 18, 23).

As mentioned previously, α_1-PI is a broad-spectrum serine proteinase inhibitor (24). GM-6001, an *N*-[2(R)-2-(hydroxamidocarbonylmethyl)-4-methylpentanoyl]-L-tryptophan methylamide, is a noncytotoxic, synthetic inhibitor that functionally and specifically inhibits MMP activity, by complexing with the zinc atom found in the active site of MMPs, and prevents substrate interaction, as described (18). 1K (ZD0892) is a peptidyl trifluoromethyl ketone with an N-terminal 4-$(CH_3O)C_6H_4CO$ group, making it an orally bioavailable serine elastase inhibitor (25). It is highly selective for neutrophil elastase (K_i = 6.7 nM), but also inhibits pancreatic elastase (K_i = 200 nM) and endogenous vascular elastase (unpublished data), but not other serine proteinases, or cysteine, or metalloproteinases. It is preferable to elafin, which is relatively unstable and must be given by continuous administration (26).

Preparation of sense and antisense vectors for transfection. A U1*Bam* pZeo mut *Eco*RI/*Spe*I expression vector backbone was a gift from H.C. Dietz and R.A. Montgomery (Johns Hopkins University School of Medicine, Baltimore, Maryland, USA) (27). Ligated into this plasmid, downstream from a constitutively active U1 promoter and between 2 snRNA hairpin loops, was a 32-bp antisense construct directed toward the 6th FN type III constant domain of rat TN (coding sequence 5′-GAAAATGCAGCCACA .... TCAGCTGGAGGGCACCG-3′) and interrupted in its middle by a 22-bp sequence (relative to TN coding sequence 5′-CAAAGCAGGAGTGCCTGAGTAG-3′) encoding a hammerhead ribozyme. Antisense target sequence selection involved maintenance of hairpin loop 2° structures and targeting of the ribozyme to mRNA containing a GUC ribozyme consensus cleavage site (Figure 1). Folding of the resultant cRNA activates the encoded ribozyme such that binding of the construct to the target TN mRNA results in cleavage of the TN mRNA at the consensus cleavage site, destabilizing it, and leading to its degradation and loss by endogenous exonuclease activity. The cRNA produced by the vector is particularly stable because of the presence of the 5′ and 3′ hairpin loops that confer resistance to exonuclease activity as a result of their high G + C content and facilitate nuclear trafficking of the construct because of lack of polyadenylation and the presence of a 5′-trimethyl guanosine cap. Sense and antisense oligonucleotides containing alternative 4-bp *Eco*RI and *Spe*I overhangs (antisense: 5′-*CTAG* GAA AAT GCA GCC ACA GTT TCG TCC TCA CGG ACT CAT CAG AGC TGG AGG GCA CCG; sense: 5′-*AATT* CGG TGC CCT CCA GCT CTG ATG AGT CCG TGA GGA CGA AAC TGT GGC TGC ATT TTC) were denatured, annealed, and ligated into the *Eco*RI and *Spe*I (Pharmacia Biotech AB, Uppsala, Sweden) linearized expression vector using T4 DNA ligase (GIBCO-BRL, Gaithersburg, Maryland, USA).

Before transfection, plasmid DNA was linearized with *Apa*I (Pharmacia) and bound to the non-histone–associated nuclear proteins, high mobility group-1 and -2 (HMG-1 and -2) (Wako Pure Chemical Industries, Osaka, Japan), to facilitate nuclear targeting of the plasmid DNA (28). The plasmid/HMG complex was enclosed in liposomes and bound with ultraviolet-inactivated hemagglutinating virus of Japan (HVJ; a kind gift from Y. Kaneda and N. Nakamura, Osaka University, Japan).

PAs were excised and both infused and incubated for 10 minutes in 250 μL of buffered saline containing 2 nM of $CaCl_2$ and 7,500 hemagglutinating units of HVJ bound to liposomes containing 50 μg of TN sense or antisense plasmid DNA or the constitutively active reporter expression plasmid pECE-CAT encoding full-length chloramphenicol acetyltransferase (CAT).

Blocking $\alpha_v\beta_3$ integrin. Hypertrophied PAs were cultured in media supplemented with either 15 μg/mL of an anti-$\alpha_v\beta_3$ functional blocking antibody, LM609 (Chemicon, Temecula, California, USA), or 15 μg/mL of control IgG (PharMingen, San Diego, California, USA), as described previously for cell culture (18).

Cell culture. Vascular SMCs were isolated from the excised PAs of Sprague-Dawley rats, and confluent cultures were collected by trypsinization and seeded on prepared collagen gels as described previously (18). Briefly, SMCs were cultured for 48 hours in medium 199 (Sigma Chemical Co.) with 0.1% BSA and 50 ng/mL epidermal growth factor (GIBCO BRL) and on gels containing either collagen alone or supplemented with 100 nM recombinant wild-type OPN expressed in *E. coli* as a glutathione S-transferase fusion protein (a kind gift from C.M. Giachelli, University of Washington, Seattle, Washington, USA) (29). Cell number was determined following collagenase digestion and counts were made using an improved Neubauer hemocytometer (American Optical, Buffalo, New York, USA). Survival was quantified as the percent of SMCs present at 48 hours relative to the number of seeded cells (cells plated – cells in medium).

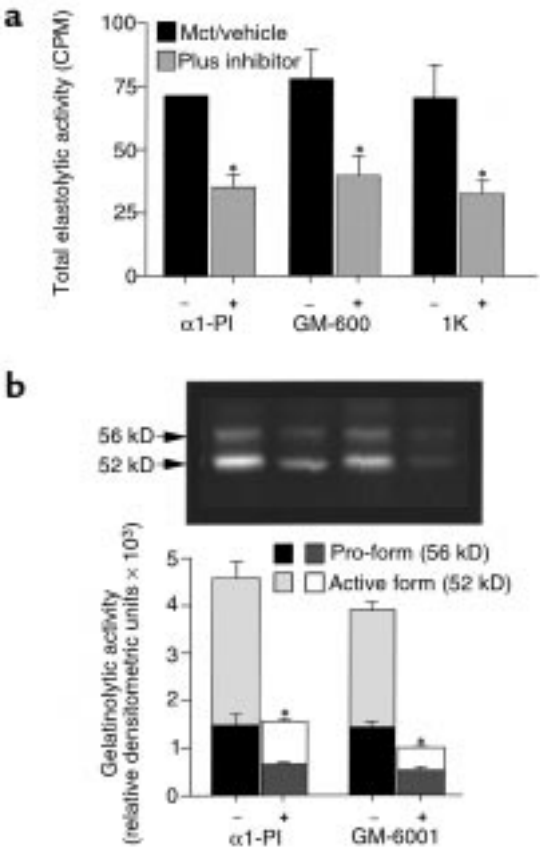

Figure 2
Elastase and MMP activity. Elastase assays were used to detect net elastolytic activity in conditioned medium harvested from 8-day-old PA cultures in the presence or absence of either the serine elastase inhibitors, α_1-PI and 1K, active against endogenous vascular elastases, or the MMP inhibitor, GM-6001 (**a**). Suppression of elastase activity was induced by all 3 inhibitors. Gelatin zymography, performed on tissue extracts of PAs grown for 8 days in media supplemented with either α_1-PI or GM-6001, or with the administration vehicle controls for each inhibitor, allowed us to see MMP activity (**b**). The most predominant bands ran as a doublet at a molecular weight of approximately 56 and 52 kD, as shown in the zymogram, representative of 3 such experiments and summarized graphically. Bars: mean + SEM ($n = 3$); $^*P < 0.05$ compared with administration vehicle controls.

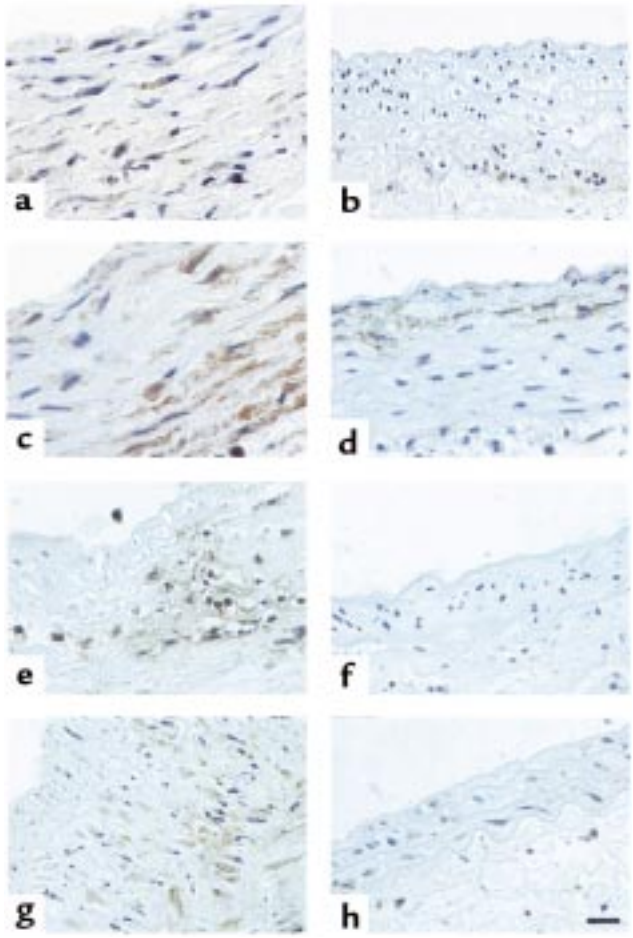

Figure 3
Regulation of TN by proteinase inhibitors. Representative photomicrographs of TN immunohistochemistry indicate that TN is increased at 21 days after Mct-injection (**a**) relative to PAs from saline-injected rats, which show only faint staining along the outer media/adventitial border (**b**). TN continues to be abundantly deposited throughout the vessel wall in vehicle-treated controls: (**c**) PBS vehicle for α_1-PI, (**e**) DMSO vehicle for GM-6001, and (**g**) PEG vehicle for 1K. In contrast, incubation with the proteinase inhibitors α_1-PI (**d**), GM-6001 (**f**), and 1K (**h**) reduces TN. Bar: 25 μm. Semi-quantitative analysis reflected these differences (not shown).

Elastase assay, and MMP activity and expression. The ability of conditioned media to degrade 200 μg of [^{3}H]-elastin was determined as described previously (22). To control for nonenzymatic degradation, radiolabeled elastin was incubated with medium cultured in the absence of tissue. Activity was related to a standard curve generated with human leukocyte elastase (0.075–5.0 ng) (Elastin Products Co., Pacific, Missouri, USA). MMP zymography was performed after homogenization of PA tissue as described previously (22) and normalized by Bradford assay to total protein (Bio-Rad Laboratories, Hercules, California, USA). MMP Western immunoblotting used an anti–MMP-2 rabbit polyclonal antisera (a kind gift from M. Silverman and M. Ailenburg, University of Toronto, Toronto, Ontario, Canada) as described previously (22).

Northern blotting for TN. Northern blot analysis was performed on 8 μg of total RNA extracted from 3 pooled PAs and hybridized to a 250-bp cDNA probe derived from the 7th FN type III constant domain of rat TN (22). TN mRNA was corrected for loading conditions by direct comparison with 28S rRNA, detected after ethidium bromide staining, and GAPDH, following hybridization with a rat-specific probe.

Immunohistochemistry and detection of apoptosis. Immunohistochemistry, using techniques described previously (22), identified TN with an anti-rat formaldehyde-fixed TN polyclonal antibody (1:100; a generous gift from H. Erickson, Duke University Medical Center, Durham, North Carolina, USA). For detection of proliferating cell nuclear antigen (PCNA), an anti-PCNA mAb (1:100) (DAKO Inc., Carpinteria, California, USA) was used. Immunohistochemistry for OPN was performed with a mAb raised against rat bone OPN, clone MPIIIB10$_1$ (11 ng/mL; Department of Biological Sciences, University of Iowa, Iowa City, Iowa, USA). FN was detected using an anti-FN mAb (1:100; Chemicon). For CAT immunostaining, an anti-CAT polyclonal antibody (1:50; 5 Prime - 3 Prime Inc., Boulder, Colorado, USA) was used. Estimates of total elastin and collagen were detected using the Movat pentachrome stain. To quantify apoptosis, TUNEL assays were performed with the ApopTag in situ detection system (Oncor Inc., Gaithersburg, Maryland, USA). Nuclear morphology was examined by labeling with propidium iodide (2 μg/mL). DNA laddering was performed as described previously (18). In the cell culture studies, apoptosis was confirmed as the mechanism for reduced cell number using the DePsipher detection system (R&D Systems Inc., Minneapolis, Minnesota, USA), which indicates loss of mitochondrial membrane potential. This assay correlates well with TUNEL and can be expediently applied to cells in culture but not readily to whole-tissue samples.

The relative abundance of the ECM components examined were graded quantitatively in 5 random fields (×400) per sample, using the Image-Pro Plus program for Macintosh (Media Cybernetics LP, Silver Spring, Maryland, USA). The program performs planimetry and densitometry on positive staining above a uniform "background" cutoff. Subsequent multiplication of both the total area positively stained and the average density of staining provides a relative densitometric unit of ECM protein content that was then averaged, and tissue means were calculated. The relative number of proliferating and apoptotic cells was quantitatively assessed in 10 randomly selected fields (×400) as a percent of total propidium iodide–stained cells.

Lactate dehydrogenase assay. Necrosis was assessed by a lactate dehydrogenase (LDH) release assay kit (Sigma Chemical Co.). Controls included tissue-free medium cultured with and without FBS, as well as supernatants from PA SMCs following freeze-thaw cycles.

Morphometric analysis of Movat pentachrome–stained sections. Twenty-five measurements of medial thickness, from

internal to external elastic lamina, were recorded over the length of each vessel, and the means were calculated.

Statistical analysis. Values from multiple experiments are expressed as mean ± SE, and statistical significance was determined using 1-way ANOVA followed by Fisher's least significant difference test of multiple comparisons to establish differences between individual groups. The number of samples in each group is indicated in the figure legends.

Results

Serine elastase and MMP inhibition and TN deposition. TN is upregulated in SMCs cultured on proteolyzed collagen and suppressed following inhibition of MMP activity (18). Increased activity of a 20-kD serine elastase (9) and MMP-2 (22) have been observed in PAs following Mct injection. We therefore addressed the effects of inhibitors of serine elastases, including endogenous vascular elastase, or of MMPs on TN expression in rat PAs 21 days after Mct injection and after 8 days in organ culture. Degradation of [^{3}H]-elastin in conditioned medium from PA organ cultures was reduced in experiments with α_1-PI, 1K, and the MMP inhibitor GM-6001 compared with their vehicle controls ($P < 0.05$) (Figure 2a). Whereas the exact nature of the enzyme in the PA responsible for the elastase activity has not been identified, it is likely the endogenous serine elastase described previously in the hypertrophied PA after Mct injection, which would be inhibited by both α_1-PI and the more selective agent, 1K. However, GM-6001 also inhibits the elastolytic activity, suggesting that there is either an equally important MMP elastolytic component or that MMPs regulate serine elastases, possibly by inactivating inhibitors (30). The elastolytic activity measured is relatively small but it may reflect only the fact that most of the secreted elastases would be bound by inhibitors such as α_2-macroglobulin or α_1-PI or tissue inhibitors of MMPs (TIMPs), which are present in the serum component of the conditioned media.

Gelatin zymography for MMP activity using tissue extracts from the same PA organ cultures detected multiple gelatinolytic bands, the most prominent of which was a doublet at approximately 56 and 50 kD (displayed in Figure 2b). This gelatinolytic doublet corresponded to MMP activity because it was suppressed by the zinc/calcium chelator EDTA and was identified by Western immunoblotting of a similar native gel to be the latent and active form of MMP-2 (data not shown). An approximately 3-fold suppression in MMP-2 activity was observed with serine elastase or MMP inhibitors compared with vehicle-treated controls ($P < 0.05$; Figure 2b). The suppression of latent MMP-2 could result from proteinase inhibition, because there would be a reduction in the ECM degradation products that normally stimulate transcription of the enzyme (31, 32). Whereas we focused on MMP-2 based on previous studies (18, 22), additional, less prominent bands were also inhibited with GM-6001 and/or EDTA, suggesting the possible involvement of other MMPs. In addition, the inhibitory profile of GM-6001 may include members of the ADAM family of proteinases (33). Taken together, our organ culture data suggest suppression of elastases and MMPs in an interdependent manner.

Deposition and localization of TN within PAs was documented by immunohistochemistry. TN accumulation was increased in association with Mct-induced PA hypertrophy (20) and deposited throughout the vessel wall (Figure 3a, relative to saline control in Figure 3b). This deposition pattern was maintained or enhanced over 8 days in organ culture in the presence of the administration vehicles for the inhibitors: PBS (Figure 3c), DMSO (Figure 3e), and PEG (Figure 3g). Proteinase inhibition by α_1-PI (Figure 3d), GM-6001 (Figure 3f), and 1K (Figure 3h) markedly reduced TN accumulation such that, with

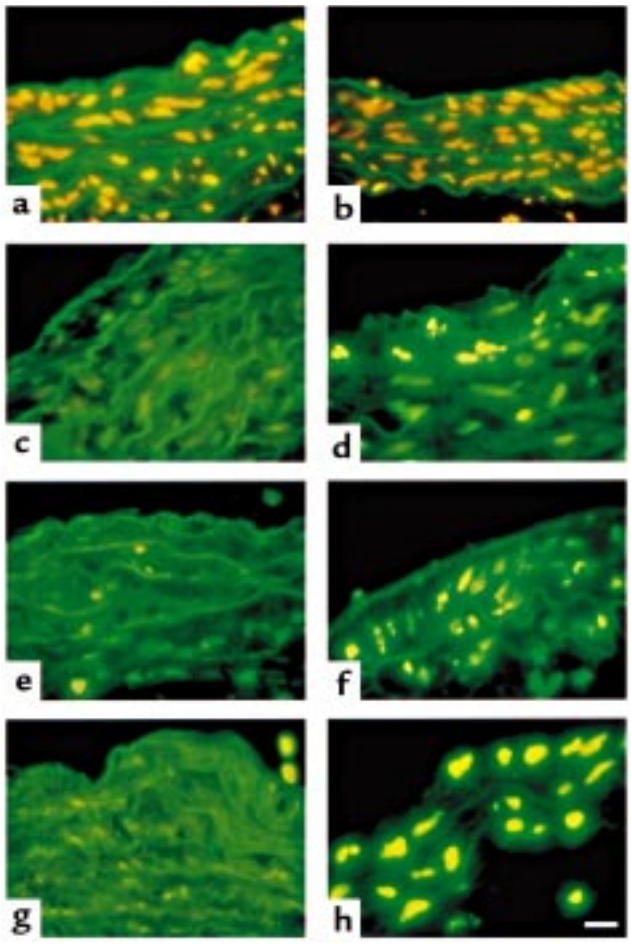

Figure 4
Apoptosis in hypertensive and normotensive PAs. Apoptotic vascular cells were identified as bright green fluorescent nuclei after TUNEL labeling. Apoptosis was minimal before culture, 21 days after either Mct (**a**) or saline injection (**b**), because only propidium iodide counterstaining can be observed. PAs cultured in media supplemented with the vehicles for the inhibitors did not show a change from preculture levels: (**c**) PBS for α_1-PI, (**e**) DMSO for GM-6001, and (**g**) PEG for 1K. However, in the presence of either α_1-PI (**d**), GM-6001 (**f**), or 1K (**h**), a widespread induction of apoptosis occurred. Bar: 25 μm.

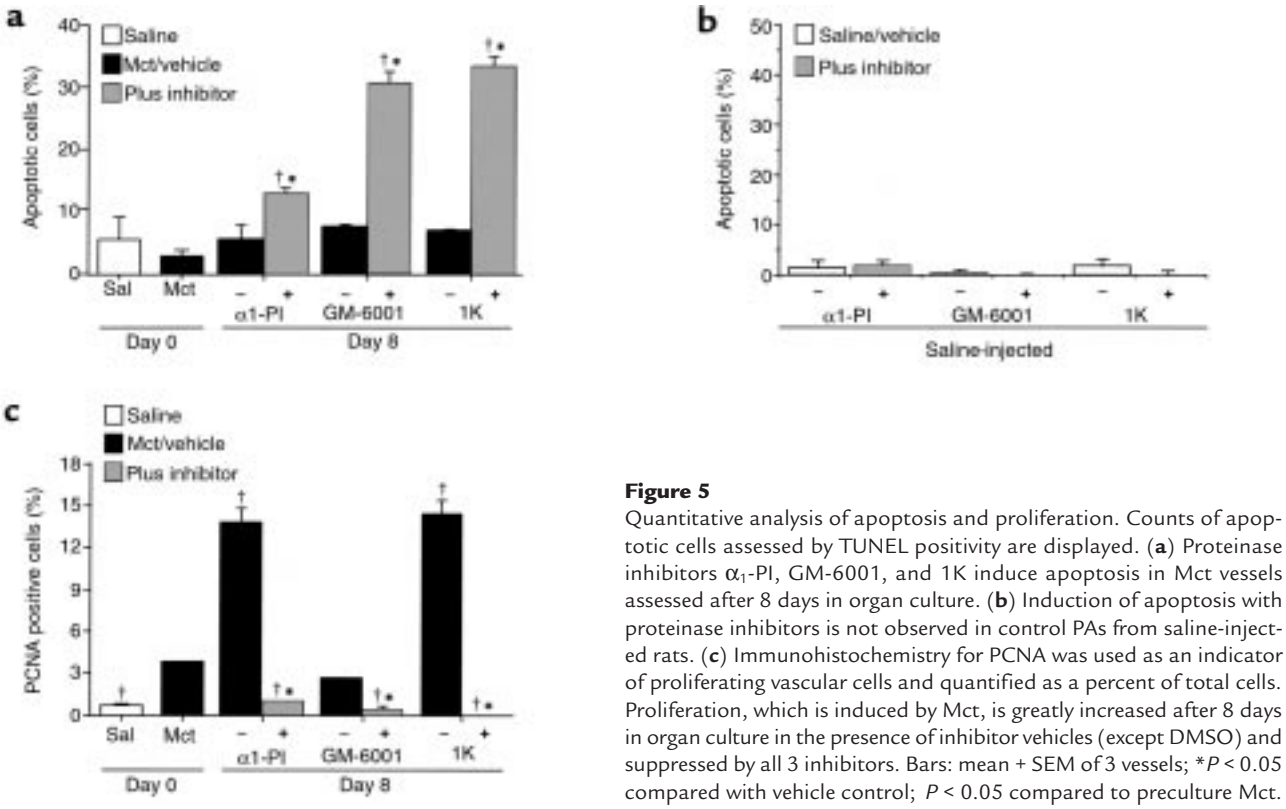

Figure 5
Quantitative analysis of apoptosis and proliferation. Counts of apoptotic cells assessed by TUNEL positivity are displayed. (**a**) Proteinase inhibitors α_1-PI, GM-6001, and 1K induce apoptosis in Mct vessels assessed after 8 days in organ culture. (**b**) Induction of apoptosis with proteinase inhibitors is not observed in control PAs from saline-injected rats. (**c**) Immunohistochemistry for PCNA was used as an indicator of proliferating vascular cells and quantified as a percent of total cells. Proliferation, which is induced by Mct, is greatly increased after 8 days in organ culture in the presence of inhibitor vehicles (except DMSO) and suppressed by all 3 inhibitors. Bars: mean + SEM of 3 vessels; $*P < 0.05$ compared with vehicle control; $P < 0.05$ compared to preculture Mct.

GM-6001 and 1K in particular, TN accumulation was severely limited. This differential deposition was confirmed by semiquantitative grading (data not shown).

Proteinase inhibition and SMC apoptosis. Previous cell culture studies have shown that suppression of TN induces SMC apoptosis (18). To provide both quantification of the number of apoptotic cells and their tissue distribution, in situ TUNEL assays were performed on PAs after 8 days of organ culture in the presence and absence of the various inhibitors (Figure 4, a–h, and Figure 5a). Less than 5% of cells were TUNEL positive at the time of organ culture, both in PAs harvested following Mct or saline control (Figure 4, a and b, respectively) injections. A similar number of TUNEL-positive cells were detected when vessels were cultured for 8 days with either PBS (Figure 4c), DMSO (Figure 4e), or PEG (Figure 4g) alone. Using α_1-PI (Figure 4d), GM-6001 (Figure 4f), and 1K (Figure 4h) all induced widespread TUNEL positivity, primarily within the vessel media, but also in the adventitia and endothelium. The percent of these cells was quantified with α_1-PI (15%), GM-6001 or 1K (30% for both), and vehicle controls (~5–7%) ($P < 0.05$; Figure 5a). The appearance of TUNEL-positive cells correlated with nuclear fragmentation and condensation. To determine whether the tissues were necrotic because of the cytotoxicity of the inhibitors, LDH assays were performed, but no enhanced activity was apparent compared with controls (data not shown).

To address the specificity of proteinase inhibition on the induction of apoptosis in Mct-treated hypertrophied PAs, we examined vessels from saline-injected rats in organ culture with media supplemented with proteinase inhibitors or their administration vehicles. TUNEL assays indicated that vascular cells from these vessels did not undergo apoptosis (Figure 5b).

Proteinase inhibition of PA organ cultures and SMC proliferation. Studies with PA SMC cultures on TN-supplemented collagen gels indicate that TN's role in disease may occur through an induction of growth-factor responsiveness in these cells (20). To determine whether modulation of TN within a 3-dimensional native vessel configuration will affect the proliferative potential of vascular cells we performed PCNA immunohistochemistry on cultured tissue (depicted in Figure 5c, photomicrographs not shown; $P < 0.05$ for each comparison). Low levels of proliferating cells, judged by PCNA positivity (~3%), were present in PAs from rats 21 days after treatment with Mct (in contrast to saline controls where values were < 1%). The further increase in PCNA positivity in organ culture was documented with vehicle-treated samples, either PBS (α_1-PI control) or PEG (1K control; ~12% for both), but not with DMSO (GM-6001 control). A reduction of PCNA positivity occurred with all 3 inhibitors: α_1-PI, GM-6001, and 1K ($P < 0.05$). Proteinase inhibitors do not influence proliferation in cultured control vessels from saline-injected rats as judged by PCNA immunostaining, which is less than 1%.

Proteinase inhibitors and regression of vessel wall hypertrophy. To determine whether regression of medial hypertrophy occurs as a result of proteinase inhibition and apoptosis, we measured PA wall thickness in Movat pen-

tachrome–stained tissue sections (Figure 6, a–h, and quantified in Figure 6i). Consistent with previous reports (8), Mct induced an increase in vessel wall thickness (Figure 6, a and i) compared with PAs derived from saline-injected rats (Figure 6, b and i). PAs cultured with administration vehicle controls continued to thicken (Figure 6, c, e, and g show PBS, DMSO, and PEG, respectively). In contrast, proteinase inhibitors showed regression of wall thickness to saline control levels with α_1-PI (Figure 6d) and to below those levels with GM-6001 (Figure 6f) and 1K (Figure 6h) (displayed graphically in Figure 6i; $P < 0.05$ for comparisons). The greatest reduction in wall thickness was observed using either the specific serine elastase or MMP inhibitors, 1K (64% reduction) and GM-6001 (45% reduction).

TN antisense and MMP activity. Because reduced TN was associated with regression of vessel wall thickness following MMP or elastase inhibition, we next addressed whether selective suppression of TN would reproduce these effects. The TN antisense expression vector was administered using the HVJ-liposome method, which facilitates a high rate of delivery to blood vessels in vivo (28). To evaluate the relative efficiency of this methodology in our model, transfections using a CAT construct were performed. Relative to mock-transfected controls (Figure 7a), abundant CAT immunostaining was observed throughout the vessel media, adventitia, and along the endothelium (Figure 7b).

TN, detected by immunohistochemistry, was present in PAs of Mct-treated rats and increased over the 8 days in organ culture with no significant difference between mock- and sense-transfected vessels ($P < 0.05$; Figure 7c, densitometric quantification). However, in PAs transfected with antisense cRNA, a significant reduction in TN deposition, to below preculture levels, was observed (56% relative to sense-transfected vessels; $P < 0.05$). The reduction in protein was attributed to antisense/ribozyme-mediated loss (58%) of both the 7.3- and 6.4-kb TN mRNA transcripts, compared with sense-transfected vessels, and observed as early as 18 hours after transfection ($P < 0.05$; Figure 7d). TN modulation by antisense was confirmed to be downstream of MMP activity because no difference in MMP-2 activity was detected (data not shown).

Antisense suppression of TN and induction of apoptosis. We next determined whether decreasing TN by antisense impairs cell survival and leads to apoptosis (Figure 8a). In freshly isolated Mct-treated PAs, apoptosis was not observed. In mock- and sense-transfected vessels, 7–10% of cells were TUNEL positive after 8 days in organ culture, but in antisense-transfected vessels, the level of apoptosis was increased to approximately 40% of cells ($P < 0.05$). We confirmed that the TUNEL-positive cells were, in fact, associated with nuclear condensation and fragmentation and DNA laddering. PAs transfected with the sense construct displayed mostly normal nuclear staining and morphology assessed by propidium iodide labeling, whereas in antisense-transfected vessels approximately 12% of nuclei exhibited

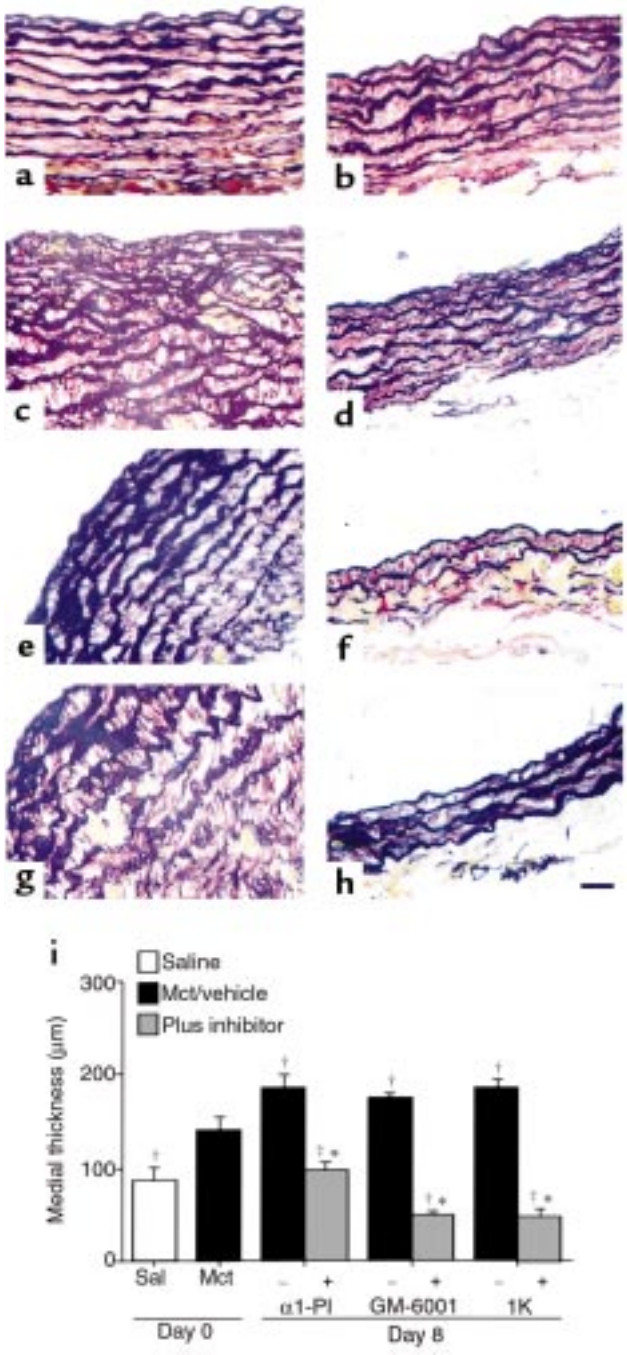

Figure 6
Proteinase inhibitors and regression of vascular hypertrophy. Representative Movat pentachrome–stained sections are shown in **a**–**h**. An increase in vessel thickness following Mct-injection (**a**), relative to that following saline-injection (**b**), but before placement into organ culture is shown. Vessels cultured in the absence of proteinase inhibition showed a further increase in wall thickness over 8 days: (**c**) PBS for α_1-PI; (**e**) DMSO for GM-6001; and (**g**) PEG for 1K. Wall thickness was reduced to or below values of saline vessels when PAs were cultured with (**d**) α_1-PI, (**f**) GM-6001, or (**h**) 1K. Whereas the size of control vehicle-treated vessels is such that they cannot be shown in entirety, differences in wall thickness are quantitatively displayed (**i**). Bar: 25 μm; graph bars: mean + SEM ($n = 6$); *$P < 0.05$ compared with vehicle control; † $P < 0.05$ compared with preculture Mct.

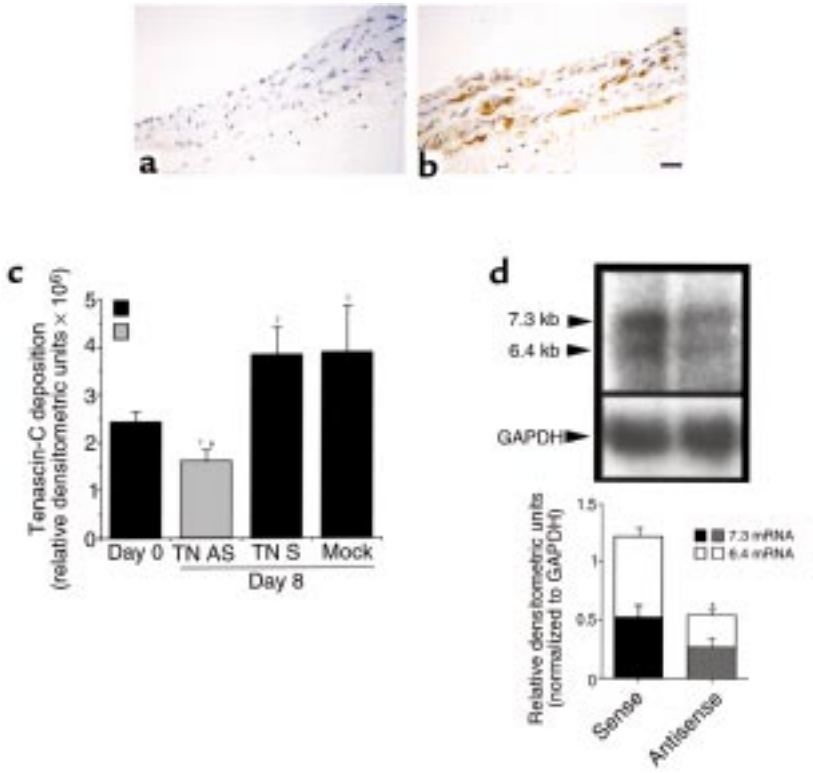

Figure 7
Distribution of TN antisense transfection and suppression of TN. Distribution of plasmid DNA following transfection was assessed indirectly by immunostaining for CAT, a gene product from another plasmid but delivered by the same HVJ-liposome technique. HVJ-liposomes are effective in transfecting the cells throughout the vessel wall ex vivo at high efficiency. Relative to IgG-stained controls (**a**), approximately 75–80% of cells are positive for CAT (**b**). Densitometric analysis of TN immunostaining (**c**) revealed an increase above preculture levels with mock or sense transfection. This was not only suppressed with TN antisense, but values were reduced below preculture levels. Reduction in TN protein assessed by immunohistochemistry correlated with decreased mRNA levels for the 2 TN transcripts as shown in the representative blot and densitometric data (**d**). With TN antisense, a decrease in TN mRNA transcripts at 7.3 and 6.4 kb was observed when normalized for hybridization and loading by GAPDH hybridization. Bar: 25 μm; graph bars: mean + SEM ($n = 4$); *$P < 0.05$ compared with sense and mock transfected; $P < 0.05$ compared with preculture Mct.

bright focal centers, indicative of DNA chromatin condensation ($P < 0.05$; Figure 8b). Nuclear fragmentation was also observed in approximately 7–8% of cells in TN antisense-transfected vessels, whereas very few such cells (< 2%) were noted in sense control PAs ($P < 0.05$; Figure 8b). DNA laddering, a hallmark of apoptosis resulting from degradation of nucleosomal DNA, was observed in sense organ cultures, but antisense transfection resulted in a 3-fold increase in intensity of these bands ($P < 0.05$; Figure 8c).

TN antisense, vascular cell proliferation, and vascular thickening. To establish whether suppression of SMC proliferation following proteinase inhibition was also observed with TN antisense, PCNA immunohistochemistry was performed (Figure 9a). A significant induction in PCNA positivity was detected above preculture levels in both the mock and sense controls, as well as with antisense transfection ($P < 0.05$ for each comparison). Thus, loss of TN by antisense failed to suppress proliferation in PA organ culture. Because suppressing TN by antisense induced apoptosis but did not arrest proliferation, the net effect on wall thickness was assessed morphometrically (quantified in Figure 9b). Whereas a significant increase in wall thickness, above day 21 controls, was observed in mock- and sense-transfected vessels ($P < 0.05$), in antisense-transfected arteries wall thickness was similar to that observed in freshly isolated, Mct-treated PAs ($P < 0.05$).

TN antisense and OPN. The presence of PCNA-positive cells in the antisense-treated PAs suggested incomplete transfection with antisense or proliferation in the absence of TN. Codistribution of TN and PCNA on serial sections was present in sense vessels (Figure 10, a, b, and e). Conversely, whereas approximately 24% of all PCNA-positive cells (Figure 10d) were associated with TN (Figure 10c) following antisense transfection, and likely represented untransfected cells, the remaining approximately 76% of cells were proliferating in a TN-independent manner (Figure 10e). Thus, antisense appeared to allow the expansion of a SMC subpopulation that is TN negative.

TN amplifies the response to growth factors by ligating β_3 integrin receptors, altering the cytoskeleton, and causing clustering and enhancing activation of growth factor receptors. OPN, another ECM molecule that contains an arginine-glycine-aspartic acid (RGD) site required to ligate β_3 integrins, mediates vascular endothelial cell survival (29) and is produced by SMCs during disease (34). We therefore investigated, using immunostaining, whether OPN was present or upregulated. The diffuse, sometimes focal, pattern of OPN deposition in sense-transfected PAs was reduced relative to preculture levels after 8 days in organ culture (Figure 11, a and e). With suppression of TN by antisense, however, OPN immunoreactivity was markedly increased and localized primarily to intense, dense foci ($P < 0.05$; Figure 11, c and e). In serial sections there appeared to be an enhanced codistribution of PCNA-positive cells with intense OPN staining in antisense vessels (Figure 11). The suppression of TN and concomitant upregulation of OPN in antisense PAs were selective effects, because other ECM molecules such as FN, elastin, and collagen were not altered in proportion to wall thickness (Figure 11e).

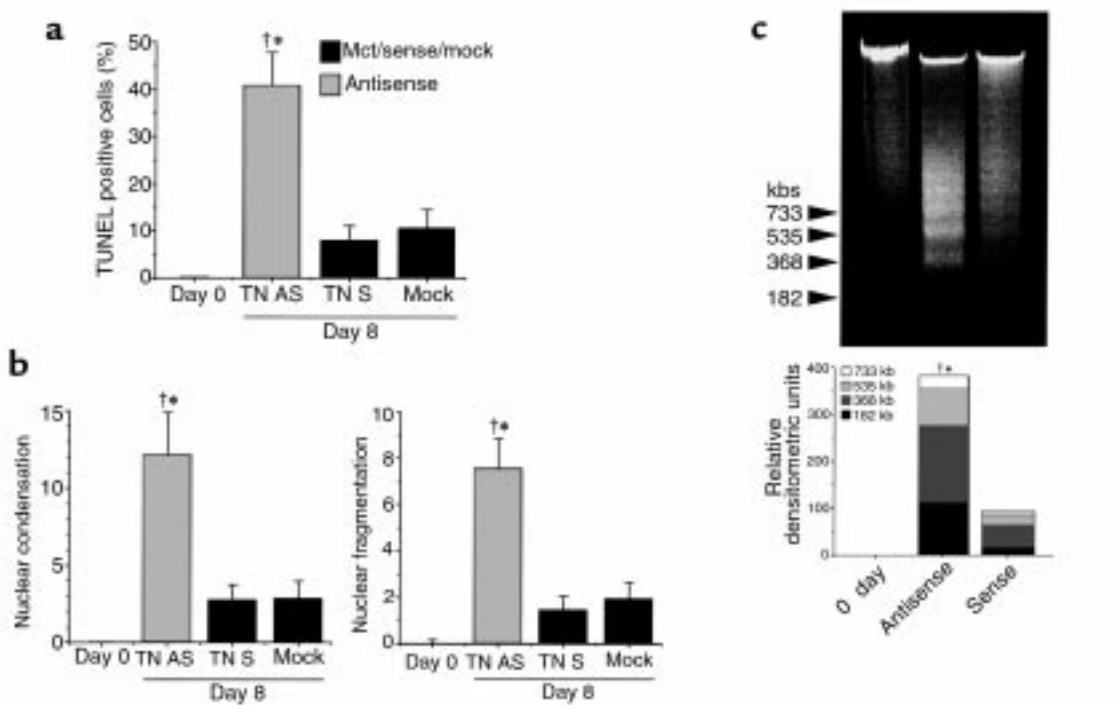

Figure 8
TN antisense transfection induces apoptosis. (**a**) The number of apoptotic vascular cells under each condition reflects a slight induction in mock- and sense-transfected PAs relative to PAs before culture. In antisense-transfected PAs, however, a marked increase was observed above these levels. To assess the stringency of TUNEL assays, additional characteristics of apoptosis were examined. DNA of cells in antisense-transfected tissue sections showed evidence of increased nuclear condensation and fragmentation quantified as a percent of total cells in (**b**). DNA laddering was seen as approximately 180-bp multimeric DNA fragments that were, by densitometry, approximately 3-fold more pronounced in antisense-transfected versus sense-transfected PAs (**c**). Extracts from PAs before culture show no evidence of such multimers. Bars: mean + SEM ($n = 4$ vessels; $n = 3$ for laddering); $^*P < 0.05$ compared with sense- and mock-transfected cells; $P < 0.05$ compared with preculture Mct.

Proteinase inhibition and OPN. Induction of OPN could account for the concomitant proliferation of SMCs resulting in arrest but not regression of PA hypertrophy, because we verified that, similar to TN, OPN expression in tissue sections from inhibitor-treated cultures (Figure 12, b and d; GM-6001 and 1K, respectively) was also reduced compared with vehicle-treated cultures (Figure 12, a and c; DMSO and PEG, respectively), as quantified in Figure 12e ($P < 0.05$).

To further explore the role of OPN as a SMC survival factor and to ensure uniform delivery of exogenous OPN, we used a PA SMC culture model characterized previously (18). We cultured rat PA SMCs with the proteinase inhibitor GM-6001, which suppresses TN (18), and showed induction of apoptosis (~50% cell loss over 48 hours), detected as DePsipher positivity as described in Methods. This rapid assay for cultured cells avoids the fixation process necessary for tissue pieces. Addition of exogenous OPN (Figure 13a), prevented the loss in cell number through the suppression of apoptosis (reduced by approximately 5-fold; $P < 0.05$).

Blockade of $\alpha_v\beta_3$ integrin, vascular cell apoptosis, and vascular regression. Because TN or OPN-dependent survival has been shown to involve the ligation of $\alpha_v\beta_3$ integrins (18, 29), we determined whether the absence of matrix interaction with this integrin could account for apoptosis and vascular regression. Hypertrophied PA organ cultures were therefore treated with the functional blocking antibody, LM609, as described in Methods. An apoptotic response was observed (~5.8-fold induction), similar to that detected with proteinase inhibitors (Figure 13e and quantified in Figure 13f), whereas untreated vessels (Figure 13c, after culture; Figure 13b, before culture) and IgG (Figure 13d) controls maintained low levels of TUNEL positivity ($P < 0.05$). This was again associated with regression of vascular hypertrophy ($P < 0.05$; Figure 13g).

Discussion

PA organ culture was used to show that inhibition of elastases and MMPs suppresses TN, and this not only arrests progression but leads to regression of the thickened vessel wall in association with apoptosis and reduction in ECM components. An antisense technique effectively suppressed TN and caused a similar degree of SMC apoptosis, but proliferation of a group of TN-negative SMCs continued unaffected in association with enhanced deposition of an alternative ECM protein survival factor, OPN. Indeed, exogenous OPN can rescue cultured SMCs from MMP-induced apoptosis associated with TN downregulation. Correspondingly, unligation of SMCs to TN and OPN by blocking the $\alpha_v\beta_3$ receptor induced apoptosis and

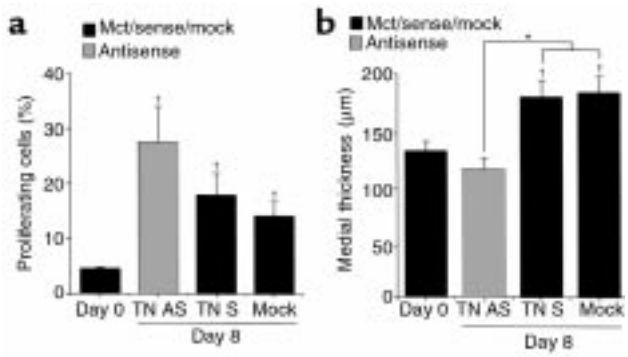

Figure 9
Effect of TN antisense on proliferation and wall thickness. (**a**) Quantification of differences in PCNA positivity indicated increased and similar levels in mock-, sense-, and antisense-treated PAs from Mct-injected rats in organ culture. (**b**) Measurements of wall thickness indicate an increase in sense and mock vessels over 8 days in culture, whereas antisense treatment results in wall thicknesses statistically similar to freshly harvested PAs. Bars: mean + SEM (n = 6 vessels; n = 4 for **a**); *P < 0.05 compared with sense and mock controls; P < 0.05 compared with preculture Mct.

regression, similar to proteinase inhibition. Taken together, this suggests that a PA SMC subpopulation is highly adaptive to survival ligand usage stimulated by the growth-promoting proteolytic environment. Thus a strategy aimed at either inhibiting the general sequelae of proteolytic events, e.g., stimulation of ECM deposition and release of growth factors, or common survival signaling pathways may be more effective in inducing regression of disease than the more selective approach of targeting a specific ECM molecule.

In this study we adapted an organ culture system used previously to show the development of a neointima in porcine aorta in association with SMC proliferation (35). Those studies showed that the mechanism of SMC proliferation is likely related to serine elastase activity (11). Serine elastases are known to stimulate SMC proliferation by releasing growth factors such as FGF-2 from ECM proteoglycans (10). Through the proteolysis of collagen, elastases can expose RGD binding sites (36), which induce β_3 integrin–dependent upregulation of the matrix glycoprotein TN (21), amplifying the SMC proliferative response by facilitating phosphorylation of growth factor receptors upon their ligation (18). In previous cell culture studies, stress unloading inhibited MMPs, suppressed TN, and induced SMC apoptosis. Recently, we showed that the response of SMCs in hypertrophied but not normal arteries to stress unloading in organ culture was similar (22). We also documented reduced elastase activity and showed that these effects translated into regression of the thickened vessel wall. It would be interesting to use available transgenic knockout mice to further explore the selective roles of MMPs, TN, and OPN. The effects observed are, however, limited to hypertrophied vessels, and Mct does not induce pulmonary vascular disease in mice.

Increased activity of both serine elastases and MMPs is associated with vascular remodeling (6, 7, 16, 17), and using either serine elastase inhibitors or MMP inhibitors over the 8 days in organ culture resulted in a similar reduction in elastase and MMP activity. It would therefore appear that progressive medial hypertrophy depends on an interaction between MMPs and serine elastases. Serine elastases could allow for activation of MMPs directly, or by inactivation of inhibitors, or vice versa. For example, if the endogenous serine elastase is similar to other elastases, such as neutrophil or pancreatic elastase, it could activate latent MMPs (12) and degrade TIMPs, and, by destabilizing TIMP-MMP complexes, facilitate release of the active enzyme (13). Elastases also release elastin or FN-derived peptides as well as ECM-incorporated FGF-2 (10), all of which can increase MMP expression and activity (14, 15, 32). Whereas elastases do not require proteolysis for activation, MMP-mediated

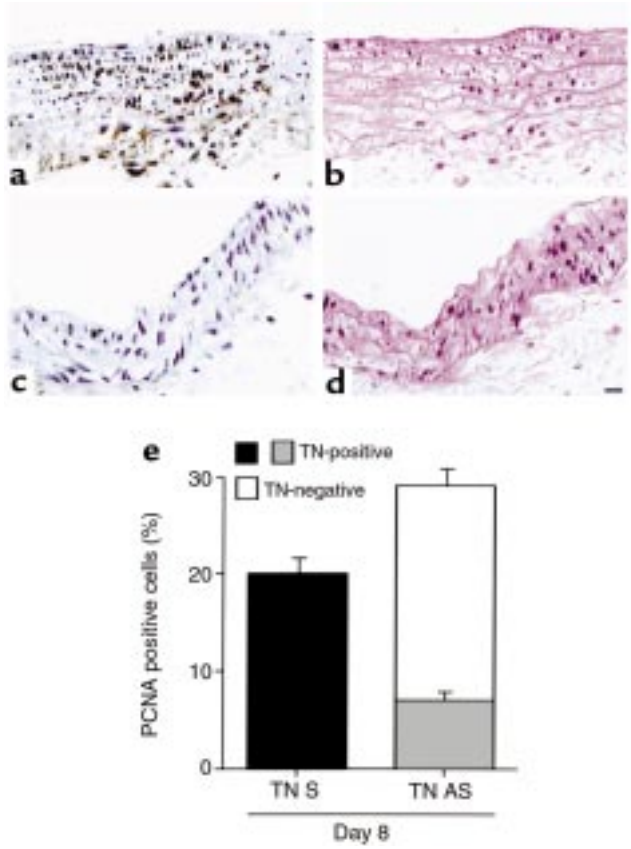

Figure 10
A TN-independent SMC population. Suppression of TN using antisense results in the expansion of a proliferating, TN-independent SMC population. Representative photomicrographs of serial sections immunostained against either TN or PCNA are shown in (**a**) and (**b**), respectively, 8 days after sense transfection, and in (**c**) and (**d**) following antisense transfection. Whereas all PCNA-positive cells were associated with TN in sense-transfected vessels, loss of TN by antisense resulted in 76% of SMCs proliferating in the absence of TN, as displayed graphically in (**e**). Bars: 25 μm; graph bars: mean + SEM of 4 vessels.

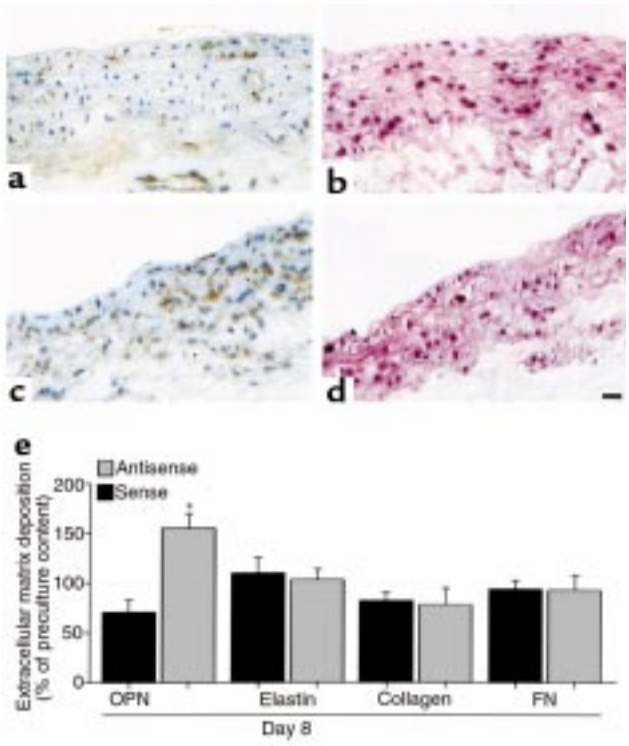

Figure 11
TN antisense induces upregulation of OPN with proliferating SMCs. The amount of OPN, an alternative $\alpha_v\beta_3$ ligand, deposited within the vessel wall was assessed. Representative photomicrographs illustrate that diffuse staining was observed in the sense control (**a**), similar to preculture observations (not shown). This was in contrast to abundant, dense focal deposition of OPN with TN antisense (**c**). The association between OPN and PCNA positivity was evident in antisense (**c**) and (**d**) relative to sense PAs (**a**) and (**b**). This increase in OPN was selectively exhibited in antisense cultures, because FN, elastin, and collagen, normalized to changes in vessel thickness, were similar [quantified in (**e**)]. Bars: 25 μm; graph bars: mean + SEM of 4 vessels; *$P < 0.05$ compared with sense control.

degradation of native elastase inhibitors, such as α_1-PI (30), may enhance vascular elastolytic activity. In addition, MMPs activated in association with endothelial injury may degrade matrix components leading to the loss of the basement membrane barrier (37) and allow serum factors to stimulate SMC elastase activity (6, 7). Alternatively, both serine elastase and MMP activities are independently associated with progressive disease, and inhibition of either serine elastase or MMP activity is sufficient to induce regression. Our previous studies examining Mct-induced PA hypertrophy attributed the elevated elastase activity to a 20-kD serine elastase (9). Matrix metalloelastases, however, were not evident, and non-elastolytic activity of MMPs was not assessed (8).

Evidence for the importance of a TN-SMC interaction in vascular biology comes from characterization of TN's tight developmental regulation and pathological re-expression (19, 20, 38). Cell culture studies have identified a number of factors that influence TN expression (39, 40), and these include MMPs that are also coinduced during vascular disease (16, 17, 19, 20). The mechanism involves proteolysis of native type I collagen and ligation of newly exposed RGD sites by β_3 integrin receptors on SMCs (18). The subsequent intracellular signaling leads to transactivation of the TN promoter (21). Furthermore, elastases can release stored matrix-bound growth factors such as FGF-2 (10), which can also stimulate production of TN (39). How inhibition of elastases, also shown recently in the intact animal (unpublished data), or MMPs (18) reduce TN expression is not known, but this may be related to suppression of the β_3 integrin–directed morphological changes and downstream signaling events described previously (21).

The mechanism whereby suppression of TN resulting either from reduced elastase or MMP activity or TN mRNA antisense leads to SMC apoptosis is not known. Because $\alpha_v\beta_3$ ligation to TN results in a reorganization of the SMC filamentous actin cytoskeleton, focal adhesion morphology, and ultimately cell-shape (18) regulating

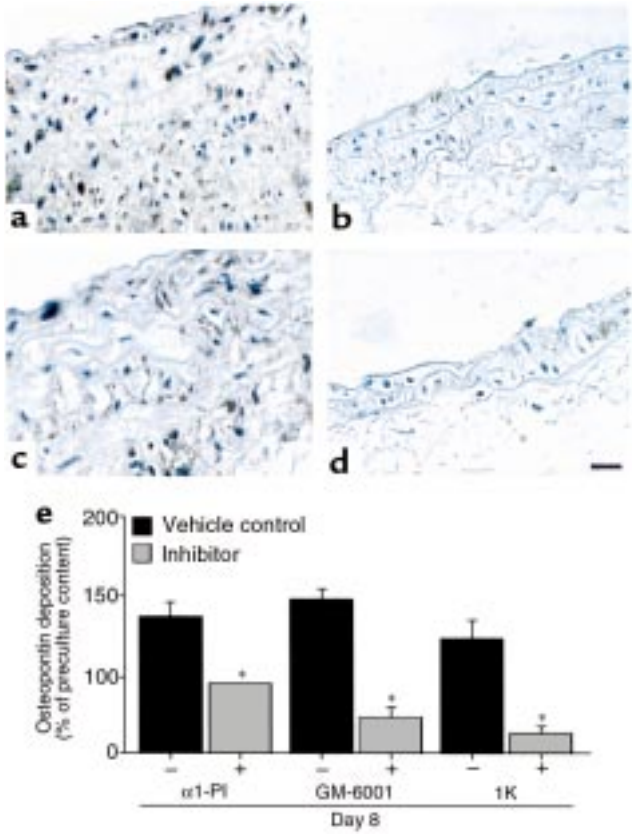

Figure 12
Suppression of OPN by proteinase inhibition and detection of OPN by immunohistochemistry in PAs cultured in the presence or absence of selective proteinase inhibitors. Representative photomicrographs indicate that whereas OPN is deposited in the absence of proteinase inhibition with vehicles (**a**) DMSO for GM-6001 and (**c**) PEG for 1K, the presence of GM-6001 (**b**) or 1K (**d**) resulted in the loss of OPN immunoreactivity. As quantified in (**e**), this retrospective examination showed that, like TN, OPN was suppressed by proteinase inhibition. Bars: 5 μm; graph bars: mean + SEM of 4 vessels; *$P < 0.05$ compared with vehicle control.

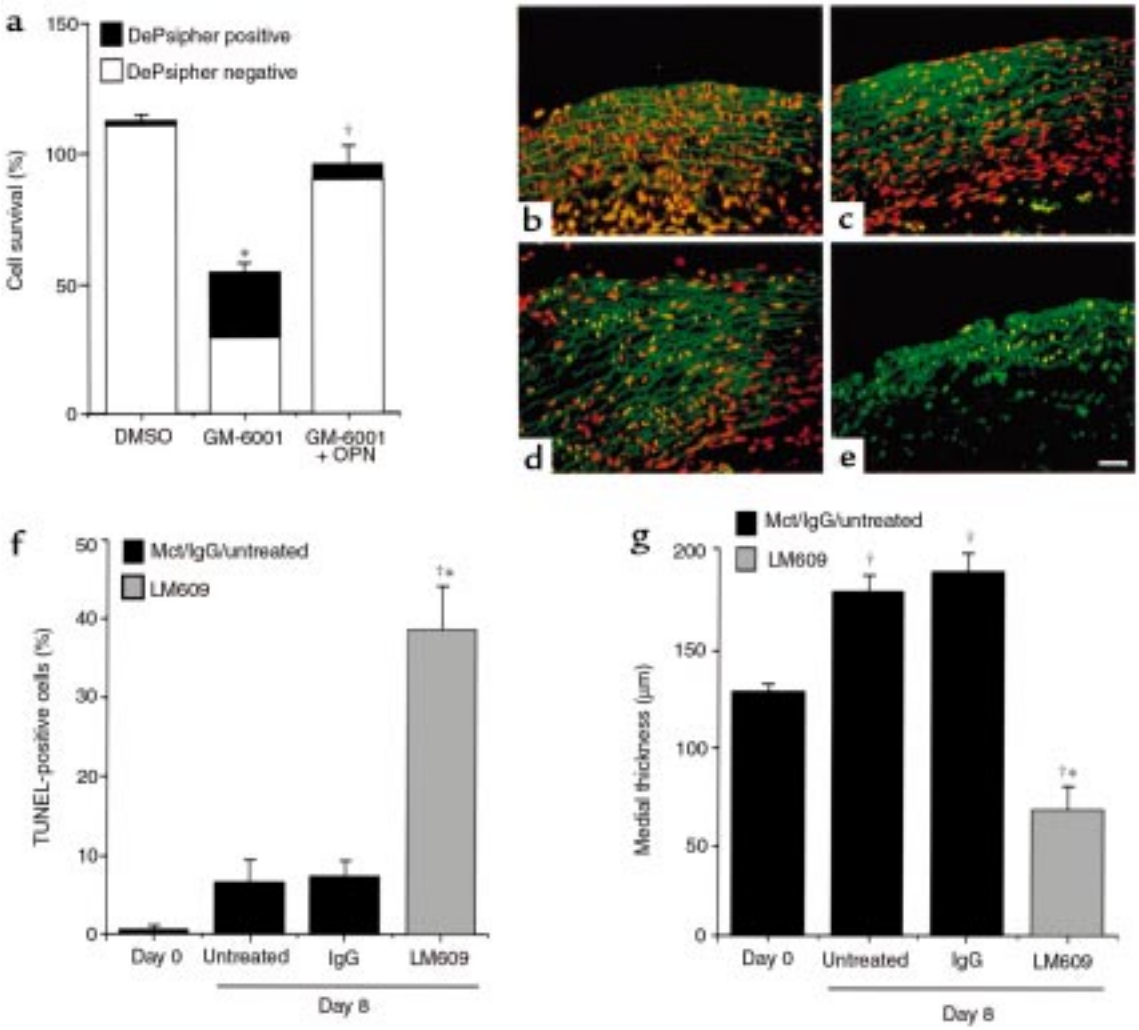

Figure 13

OPN- and $\alpha_v\beta_3$-mediated SMC survival. (**a**) Effect of exogenous OPN on apoptosis of rat PA SMCs following MMP inhibition associated with loss of the SMC survival ligand TN. The addition of recombinant OPN to collagen gels prevented loss of cell number and rescued the SMCs from apoptosis, as assessed by loss of mitochondrial membrane potential (DePsipher positivity) described in Methods. Next we investigated the effect of $\alpha_v\beta_3$ integrin blockade in inducing apoptosis in hypertrophied PA organ cultures. Representative photomicrographs indicate that whereas apoptosis (bright green TUNEL-positive fluorescent nuclei) was minimal or absent in PAs after Mct injection both before culture, day 21 (**b**), and after 1 week of culture, either untreated (**c**) or treated with control IgG (**d**), unligation of the $\alpha_v\beta_3$ integrin with LM609 antibodies resulted in an abundant apoptotic response (**e**). This apoptosis, quantified in (**f**), was associated with regression of vascular hypertrophy as evident in the photomicrographs and as quantified in (**g**). Bars: 25 μm; graph bars: mean + SEM of 4 dishes or vessels; $^*P < 0.05$ compared with DMSO control in **a** and IgG control in **f** and **g**; $P < 0.05$ compared with GM-6001 in **a** and preculture Mct (day 0) in **f** and **g**.

cell behavior (41, 42), loss of this ligation to TN may initiate the apoptotic cascade. Correspondingly, apoptosing cells can be rescued by addition of exogenous TN (18). Our studies documenting induction of SMC apoptosis with an $\alpha_v\beta_3$ functional blocking antibody would support suppression of $\alpha_v\beta_3$ ligation as the mechanism.

We further suggest that if SMCs respond similarly to endothelial cells, $\alpha_v\beta_3$ ligation may involve nuclear factor-κB–related (NF-κB–related) signaling (29). This involvement would lead to transcriptional activation of inhibitor of apoptosis protein (IAP-1; ref. 43), together with sustained extracellular signal-related kinase (ERK) activity (44) and suppression of p53 and the cyclin-dependent kinase inhibitor $p21^{WAF1/CIP1}$ (45). Similar to our studies with cultured SMCs, blocking endothelial cell $\alpha_v\beta_3$ integrin interactions with either cyclic peptides or functional blocking antibodies induces apoptosis leading to vessel loss (46, 47). Moreover, an $\alpha_v\beta_3$ integrin survival signal within the vasculature has been further supported by α_v knockout mice, which exhibit an embryonically lethal phenotype (48). Whereas evidence for an $\alpha_v\beta_3$-TN SMC survival pathway is strong, as provided by this report and others (18), these studies appear, at first, to be inconsistent with the presence of only a mild phenotype when TN is knocked out (49). Reconciliation of these facts is likely to involve the presence of redundant cell survival signals, as our present data suggests, such as coordinate upregulation of OPN, an alternative $\alpha_v\beta_3$ integrin ligand.

OPN is expressed by SMCs present in vascular disease (34), and its role as a survival factor has been reported in endothelial cells (29). We have now shown that exogenous OPN can also support survival of SMCs when proteinase inhibition suppresses ECM survival ligands. Indeed, failure to expand a proliferative, TN-negative subpopulation following proteinase inhibition correlated with loss of both TN and OPN. The possibility exists that OPN expression by SMCs is enhanced by proteinase activity enabling them to respond to pro-proliferative cues. Although we have not identified other characteristics that differentiate the TN-dependent SMCs that apoptose following TN antisense treatment from the TN-independent cells that produce increased OPN, these results are in keeping with recent work by Frid and colleagues (50) documenting heterogeneity of PA SMCs. Such heterogeneous populations suggest the potential for an adaptive response to alterations in cell matrix interactions in disease.

In our study regression of hypertrophy involved both a loss of cellular and matrix components, whereas previous studies have addressed only a requirement for a reduction in cellularity (51). Loss of ECM, paradoxically in the presence of proteinase inhibitors, may have resulted from phagocytosis and intracellular degradation by vascular cells (52). Matrix degradation within vesicular membranes would have been inaccessible to the inhibitors used in our study. Alternatively, proteolysis of ECM may have been the effect of enzymes not targeted by the inhibitors used in our study, e.g., by release of upregulated apoptosis-associated enzymes with ECM-degrading capacities into the microenvironment (53).

These organ culture studies have suggested a novel strategy to induce regression of vascular disease. Proteinase inhibitors produce a robust apoptotic response accompanied by loss of ECM, whereas the heterogeneity and plasticity of vascular SMC subpopulations appear to limit the usefulness of targeting specific ECM survival factors.

Acknowledgments

This work was supported by the Heart and Stroke Foundation of Canada Grant HSFO 3170 and the Primary Pulmonary Hypertension Cure Foundation. M. Rabinovitch is a chair of the Heart and Stroke Foundation of Canada. K.N. Cowan holds a K.M. Hunter/Medical Research Council of Canada doctoral fellowship. We are indebted to L. Morikawa and R. Johns of the Pathology Department at The Hospital for Sick Children. We would also like to thank J. Jowlabar and J. Matthews for their help in preparing this manuscript, as well as the members of our laboratory for their suggestions during the course of this study.

1. Rabinovitch, M. 1998. Diseases of the pulmonary vasculature. In *Comprehensive cardiovascular medicine*. E.J. Topol, editor. Lippincott-Raven Publishers. Philadelphia, PA. 3001–3029.
2. Meyrick, B., and Reid, L. 1980. Ultrastructural findings in lung biopsy material from children with congenital heart defects. *Am. J. Pathol.* **101**:527–537.
3. Prosser, I., et al. 1989. Regional heterogeneity of elastin and collagen gene expression in intralobar arteries in response to hypoxic pulmonary hypertension as demonstrated by in situ hybridization. *Am. J. Pathol.* **135**:1073–1088.
4. Jones, P.L., Cowan, K., and Rabinovitch, M. 1997. Tenascin-C, proliferation and subendothelial accumulation of fibronectin in progressive pulmonary vascular disease. *Am. J. Pathol.* **150**:1349–1360.
5. Rabinovitch, M., et al. 1986. Pulmonary artery endothelial abnormalities in patients with congenital heart defects and pulmonary hypertension: a correlation of light with scanning electron microscopy and transmission electron microscopy. *Lab. Invest.* **55**:632–653.
6. Wigle, D., et al. 1998. Aml-1 like transcription factor induces serine elastase activity in bovine pulmonary artery smooth muscle cells. *Circ. Res.* **83**:252–263.
7. Thompson, K., Kobayashi, J., Childs, T., Wigle, D., and Rabinovitch, M. 1998. Endothelial and serum factors which include apolipoprotein A1 tether elastin to smooth muscle cells inducing serine elastase activity via tyrosine kinase-mediated transcription and translation. *J. Cell Physiol.* **174**:78–89.
8. Todorovich-Hunter, L., et al. 1992. Increased pulmonary artery elastolytic activity in adult rats with monocrotaline-induced progressive hypertensive pulmonary vascular disease compared with infant rats with nonprogressive disease. *Am. Rev. Respir. Dis.* **146**:213–223.
9. Zhu, L., et al. 1994. The endogenous vascular elastase that governs development and progression of monocrotaline-induced pulmonary hypertension in rats is a novel enzyme related to the serine proteinase adipsin. *J. Clin. Invest.* **94**:1163–1171.
10. Thompson, K., and Rabinovitch, M. 1995. Exogenous leukocyte and endogenous elastases can mediate mitogenic activity in pulmonary artery smooth muscle cells by release of extracellular matrix-bound basic fibroblast growth factor. *J. Cell. Physiol.* **166**:495–505.
11. Oho, S., et al. 1995. Increased elastin-degrading activity and neointimal formation in porcine aortic organ culture. Reduction of both features with a serine proteinase inhibitor. *Arterioscler. Thromb. Vasc. Biol.* **15**:2200–2205.
12. Okada, Y., and Nakanishi, I. 1989. Activation of matrix metalloproteinase-3 (stromelysin) and matrix metalloproteinase-2 ("gelatinase") by human neutrophil elastase and cathepsin G. *FEBS Lett.* **249**:353–356.
13. Itoh, Y., and Nagase, H. 1995. Preferential inactivation of tissue inhibitor of metalloproteinases-1 that is bound to the precursor of matrix metalloproteinase-9 (progelatinase B) by human neutrophil elastase. *J. Biol. Chem.* **270**:16518–16521.
14. Landeau, J.M., Pellat, B., and Hornebeck, W. 1994. Increased secretion of latent elastase activity following contact between human skin fibroblasts and elastin derived peptides. *Cell Biol. Int.* **18**:111–117.
15. Miyake, H., et al. 1997. Basic fibroblast growth factor regulates matrix metalloproteinase production and *in vitro* invasiveness in human bladder cancer cell lines. *J. Urol.* **157**:2351–2355.
16. Patel, M.I., Melrose, J., Ghosh, P., and Appleberg, M. 1996. Increased synthesis of matrix metalloproteinases by aortic smooth muscle cells is implicated in the etiopathogenesis of abdominal aortic aneurysms. *J. Vasc. Surg.* **24**:82–92.
17. Zempo, N., Kenagy, R., Bendeck, M., Clowes, M., and Reidy, M. 1994. Matrix metalloproteinases of vascular smooth muscle cells are increased in balloon-injured rat carotid arteries. *J. Vasc. Surg.* **20**:209–217.
18. Jones, P.L., Crack, J., and Rabinovitch, M. 1997. Regulation of tenascin-C, a vascular smooth muscle cell survival factor that interacts with the αvβ3 integrin to promote epidermal growth factor receptor phosphorylation and growth. *J. Cell Biol.* **139**:279–293.
19. Hedin, U., Holm, J., and Hansson, G.K. 1991. Induction of tenascin-C in rat arterial injury: relationship to altered smooth muscle cells phenotype. *Am. J. Pathol.* **139**:649–656.
20. Jones, P.L., and Rabinovitch, M. 1996. Tenascin-C is induced with progressive pulmonary vascular disease in rats and is functionally related to increased smooth muscle cell proliferation. *Circ. Res.* **79**:1131–1142.
21. Jones, P.L., Jones, F.S., Zhou, B., and Rabinovitch, M. 1999. Denatured type I collagen induction of vascular smooth muscle cell tenascin-C gene expression is dependent upon a β3 integrin-mediated mitogen-activated protein kinase pathway and a 122 base pair promoter element. *J. Cell Sci.* **112**:435–445.
22. Cowan, K.N., Jones, P.L., and Rabinovitch, M. 1999. Regression of hypertrophied rat pulmonary arteries in organ culture is associated with suppression of proteolytic activity, inhibition of tenascin-C, and smooth muscle cell apoptosis. *Circ. Res.* **84**:1223–1233.
23. Lee, J.-K., et al. 1998. A serine elastase inhibitor reduces inflammation and fibrosis and preserves cardiac function after experimentally-induced murine myocarditis. *Nat. Med.* **4**:1383–1391.
24. Beatty, K., Bieth, J., and Travis, J. 1980. Kinetics of association of serine proteinases with native and oxidized alpha-1-proteinase inhibitor and alpha-1-antichymotrypsin. *J. Biol. Chem.* **255**:3931–3934.
25. Edwards, P.D., et al. 1997. Discovery and biological activity of orally active peptidyl trifluoromethyl ketone inhibitors of human neutrophil elastase. *J. Med. Chem.* **40**:1876–1885.

26. Cowan, B., et al. 1996. Elafin, a serine elastase inhibitor, attenuates postcardiac transplant coronary arteriopathy and reduces myocardial necrosis is rabbits after heterotopic cardiac transplantation. *J. Clin. Invest.* **97**:2452–2468.
27. Montgomery, R.A., and Dietz, H.C. 1997. Inhibition of fibrillin 1 expression using U1 snRNA as a vehicle for the presentation of antisense targeting sequence. *Hum. Mol. Genet.* **6**:519–525.
28. Yonemitsu, Y., et al. 1996. Characterization of in vivo gene transfer into the arterial wall mediated by the Sendai virus (haemagglutinating virus of Japan) liposomes: an effective tool for the in vivo study of arterial diseases. *Lab. Invest.* **75**:313–323.
29. Scatena, M., et al. 1998. NF-kappaB mediates alpha v beta 3 integrin-induced endothelial cell survival. *J. Cell Biol.* **141**:1083–1093.
30. Mast, A.E., et al. 1991. Kinetics and physiologic relevance of the inactivation of alpha 1-proteinase inhibitor, alpha 1-antichymotrypsin, and antithrombin III by matrix metalloproteinase-1 (tissue collagenase), -2 (72-kDa gelatinase/type IV collagenase), and -3 (stromelysin). *J. Biol. Chem.* **266**:15810–15816.
31. Huhtala, P., et al. 1995. Cooperative signaling by alpha 5 beta 1 and alpha 4 beta 1 integrins regulates metalloproteinase gene expression in fibroblasts adhering to fibronectin. *J. Cell Biol.* **129**:867–879.
32. Werb, Z., Tremble, P.M., Behrendtsen, O., Crowley, E., and Damsky, C.H. 1989. Signal transduction through the fibronectin receptor induces collagenase and stromelysin gene expression. *J. Cell Biol.* **109**:877–889.
33. Amour, A., et al. 1998. TNF-alpha converting enzyme (TACE) is inhibited by TIMP-3. *FEBS Lett.* **435**:39–44.
34. O'Brien, E.R., et al. 1994. Osteopontin is synthesized by macrophage, smooth muscle, and endothelial cells in primary and restenotic human coronary atherosclerotic plaques. *Arterioscler. Thromb. Vasc. Biol.* **14**:1648–1656.
35. Koo, E.W., and Gotlieb, A.I. 1991. Neointimal formation in the porcine aortic organ culture. I. Cellular dynamics over 1 month. *Lab. Invest.* **64**:743–753.
36. Kafienan, W., Buttle, D.J., Burnette, D., and Hollander, A.P. 1998. Cleavage of native type I collagen by human neutrophil elastase. *Biochem. J.* **330**:897–902.
37. Emonard, H., and Hornebeck, W. 1997. Binding of 92 kDa and 72 kDa progelatinases to insoluble elastin modulates their proteolytic activation. *Biol. Chem.* **378**:265–271.
38. Kostianovsky, M., Greco, M.A., Cangiarella, J., and Zagzag, D. 1997. Tenascin-C expression in ultrastructurally defined angiogenic and vasculogenic lesions. *Ultrastruct. Pathol.* **21**:537–544.
39. Rettig, W.J., Erickson, H.P., Albino, A.P., and Garin-Chesa, P. 1994. Induction of human tenascin (neuronectin) by growth factors and cytokines: cell type-specific signals and signalling pathways. *J. Cell Sci.* **107**:487–497.
40. Chiquet-Ehrismann, R., et al. 1994. Tenascin-C expression by fibroblasts is elevated in stressed collagen gels. *J. Cell Biol.* **127**:2093–2101.
41. Chen, C.S., Mrksich, M., Huang, S., Whitesides, G.M., and Ingber, D.E. 1997. Geometric control of cell life and death. *Science.* **276**:1425–1428.
42. Folkman, J., and Moscona, A. 1978. Role of cell shape in growth control. *Nature.* **273**:345–349.
43. Erl, W., et al. 1999. Nuclear factor-κB regulates induction of apoptosis and inhibitor of apoptosis protein-1 expression in vascular smooth muscle cells. *Circ. Res.* **84**:668–677.
44. Eliceiri, B.P., Klemke, R., Stromblad, S., and Cheresh, D.A. 1998. Integrin αvβ3 requirement for sustained mitogen-activated protein kinase activity during angiogenesis. *J. Cell Biol.* **140**:1255–1263.
45. Stromblad, S., Becker, J.C., Yebra, M., Brooks, P.C., and Cheresh, D.A. 1996. Suppression of p53 activity and $p21^{WAF1/CIP1}$ expression by vascular cell integrin αvβ3 during angiogenesis. *J. Clin. Invest.* **98**:426–433.
46. Choi, E.T., et al. 1994. Inhibition of neointimal hyperplasia by blocking alpha V beta 3 integrin with a small peptide antagonist GpenGRGDSPCA. *J. Vasc. Surg.* **19**:125–134.
47. Brooks, P.C., et al. 1994. Integrin alpha v beta 3 antagonists promote tumor regression by inducing apoptosis of angiogenic blood vessels. *Cell.* **79**:1157–1164.
48. Bader, B.L., Rayburn, H., Crowley, D., and Hynes, R.O. 1998. Extensive vasculogenesis, angiogenesis, and organogenesis precede lethality in mice lacking all alpha v integrins. *Cell.* **95**:507–519.
49. Saga, Y., Yagi, T., Ikawa, Y., Sakakura, T., and Aizawa, S. 1992. Mice develop normally without tenascin. *Genes Dev.* **6**:1821–1831.
50. Frid, M.G., Aldashev, A.A., Dempsey, E.C., and Stenmark, K.R. 1997. Smooth muscle cells isolated from discrete compartments of the mature vascular media exhibit unique phenotypes and distinct growth capabilities. *Circ. Res.* **81**:940–952.
51. Pollman, M.J., Hall, J.L., Mann, M.J., Zhang, L., and Gibbons, G.H. 1998. Inhibition of neointimal cell bcl-x expression induces apoptosis and regression of vascular disease. *Nat. Med.* **4**:222–227.
52. Sawada, T., and Inoue, S. 1997. High resolution ultrastructural study of resorption of elastin fibers by fibroblasts in monkey gingiva. *Mol. Biol. Cell.* **8**(Suppl.):66a. (Abstr.)
53. Ormerod, M.G., et al. 1993. Increased membrane permeability of apoptotic thymocytes: a flow cytometric study. *Cytometry.* **14**:595–602.